Chapter 6

The KL transform and eigenimages

In this chapter we will discuss another technique to improve the information content of seismic data. The application of eigenimage analysis in seismology was proposed by Hemon and Mace (1978). In their approach they use a particular linear transformation called the Karhunen-Loeè (KL) transformation. The KL trnsormation is also knows as the principal component transformation, the eigenvector transfomation or the Hotelling transofmation. Of particular relevance to the ensuing discussion is the excellent paper by Ready and Vintz (1973) which deals with information extraction and SNR improvement in multispectral imagery.

In 1983, the work of Hemon and Mace was extended by a group of researchers at the University of British Columbia in Canada which culminated in the work of Jones and Levy (1987).

In 1988 Freire and Ulrych applied the KL transformation in a somewhat different manner to the processing of vertical seismic profiling data. The actual approach which was adopted in this work was by means of singular value decomposition (SVD), which is another way of viewing the KL transformation (the relationship between the KL and SVD transformations is discussed in this chapter).

A seismic section which consists of M traces with N points per trace may be viewed as a data matrix $\mathbf{X}$ where each element x_{ij} represents the i^{th} point of the j^{th} trace. A singular value decomposition (Lanczos, 1961), decomposes $\mathbf{X}$ into a weighted sum of orthogonal rank one matrices which have been designated by Andrews and Hunt (1977) as eigenimages of $\mathbf{X}$. A particularly useful aspect of the eigenimage decomposition is its application in the complex form. In this instance, if each trace is transformed into the analytic form, then the eigenimage processing of the complex data matrix allows both time and phase shifts to be considered which is of particular importance in the case of the correction of residual statics.

6.1 Mathematical framework

We consider the data matrix $\mathbf{X}$ to be composed of M traces with N data points per trace, the M traces forming the rows of $\mathbf{X}$. The SVD of $\mathbf{X}$ is given by, (Lanczos (1961)),

$$\mathbf{X} = \sum_{\mathbf{i=1}}^{\mathbf{r}} \sigma_\mathbf{i} \mathbf{u_i} \mathbf{v_i^T}. \tag{6.1}$$

where ^{T} indicates transpose, r is the rank of $\mathbf{X}$, $\mathbf{u}_i$ is the ith eigenvector of $\mathbf{XX^T}$, $\mathbf{v}_i$ is the ith eigenvector of $\mathbf{X^TX}$ and σ_i is the ith singular value of $\mathbf{X}$. The singular values σ_i can be shown to be the positive square roots of the eigenvalues of the matrices $\mathbf{XX^T}$ and $\mathbf{X^TX}$. These eigenvalues are always positive owing to the positive definite nature of the matrices $\mathbf{XX^T}$ and $\mathbf{X^TX}$. In matrix form equation (6.1) is written as

$$\mathbf{X} = \mathbf{U\Sigma V^T} \tag{6.2}$$

Andrews and Hunt (1977) designate the outer dot product $\mathbf{u}_i\mathbf{v}_i^T$ as the ith eigenimage of the matrix $\mathbf{X}$. Owing to the orthonormality of the eigenvectors, the eigenimages form an orthonormal basis which may be used to reconstruct $\mathbf{X}$ according to equation (6.1).

Suppose, for example, that $\mathbf{X}$ represents a seismic section and that all M traces are linearly independent. In this case $\mathbf{X}$ is of full rank M, all the σ_i are different from zero and a perfect reconstruction of $\mathbf{X}$ requires all eigenimages. On the other hand, in the case where all M traces are equal to within a scale factor, all traces are linearly dependent, $\mathbf{X}$ is of rank one and may be perfectly reconstructed by the first eigenimage $\sigma_1\mathbf{u_1}\mathbf{v_1^T}$. In the general case, depending on the linear dependence which exists among the traces, $\mathbf{X}$ may be reconstructed from only the first few eigenimages. In this case, the data may be considered to be composed of traces which show a high degree of trace-to-trace correlation. Indeed, $\mathbf{XX^T}$ is, of course, a weighted estimate of the zero lag covariance matrix of the data $\mathbf{X}$ and the structure of this covariance matrix, particularly the distribution of the magnitudes of the corresponding eigenvalues, indicates the parsimony or otherwise of the eigenimage decomposition. If only $p, p < r$, eigenimages are used to approximate $\mathbf{X}$, a reconstruction error ϵ is given by

$$\epsilon = \sum_{k=p+1}^{r} \sigma_k^2 \,. \tag{6.3}$$

Freire and Ulrych (1988) defined band-pass $\mathbf{X_{BP}}$, low-pass $\mathbf{X_{LP}}$ and high-pass $\mathbf{X_{HP}}$

eigenimages in terms of the ranges of singular values used. The band-pass image is reconstructed by rejecting highly correlated as well as highly uncorrelated traces and is given by

$$\mathbf{X_{BP}} = \sum_{\mathbf{i=p}}^{\mathbf{q}} \sigma_\mathbf{i} \mathbf{u_i} \mathbf{v_i^T}\,, \qquad \mathbf{1 < p \leq q < r}\,. \tag{6.4}$$

The summation for X_{LP} is from $i = 1$ to $p - 1$ and for $\mathbf{X_{HP}}$ from $i = q + 1$ to r. It may be simply shown that the percentage of the energy which is contained in a reconstructed image X_{BP} is given by E, where

$$E = \frac{\sum_{i=p}^{q} \sigma_i^2}{\sum_{i=1}^{r} \sigma_i^2}\,. \tag{6.5}$$

The choice of p and q depends on the relative magnitudes of the singular values, which are a function of the input data. These parameters may, in general, be estimated from a plot of the eigenavalues $\lambda_i = \sigma_i^2$ as a function of the index i. In certain cases, an abrupt change in the eigenvalues is easily recognised. In other cases, the change in eigenvalue magnitude is more gradual and care must be exercised in the choice of the appropriate index values.

In Figures 6.1 and 6.2 we illustrate the reconstruction fo a flat event immersed in noise using the first eigenimage of the data. In this example only the most energetic singular value was retained. When the data exhibit some type of moveout, one eigenimage is not sufficient to properly reconstruct the data. This can be observed in Figures 6.3 and 6.4.

As we have seen, decomposition of an image $\mathbf{X}$ into eigenimages is performed by means of the SVD of $\mathbf{X}$. Many authors also refer to this decomposition as the Karhunen-Loève or KL transformation. We believe however, that the SVD and KL approaches are not equivalent theoretically for image processing and, in order to avoid confusion, we suggest the adoption of the term eigenimage processing. Some clarification is in order.

A wide sense stationary process $\xi(t)$ allows the expansion

$$\widehat{\xi}(t) = \sum_{n=1}^{\infty} c_n \psi_n(t) \quad 0 < t < T \tag{6.6}$$

where $\psi_n(t)$ is a set of orthonormal functions in the interval $(0, T)$ and the coefficients c_n are random variables. The Fourier series is a special case of the expansion given by equation (6.6) and it can be shown that, in this case, $\xi(t) = \widehat{\xi}(t)$ for every t and the

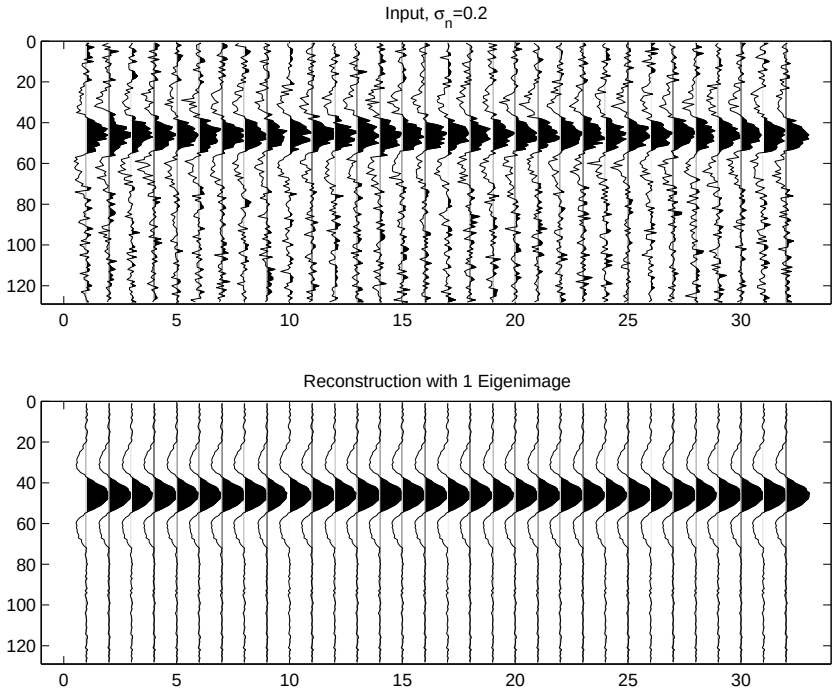

Figure 6.1: A flat event immersed in nose and the recostruction by means of the first eigenimage

coefficients c_n are uncorrelated only when $\xi(t)$ is mean squared periodic. Otherwise, $\xi(t) = \widehat{\xi}(t)$ only for $|t| < T/2$ and the coefficients c_n are no longer uncorrelated. In order to guarantee that the c_n are uncorrelated and that $\xi(t) = \widehat{\xi}(t)$ for every t without the requirement of mean squared periodicity, it turns out that the $\psi_n(t)$ must be determined from the solution of the integral equation

$$\int_0^T R(t_1,t_2)\psi(t_2)dt_2 = \lambda\psi(t_1) \quad 0 < t_1 < T \tag{6.7}$$

where $R(t_1,t_2)$ is the autocovariance of the process $\xi(t)$.

Substituting the eigenvectors which are the solutions of equation (6.7) into equation (6.6) gives the KL expansion of $\xi(t)$. An infinite number of basis functions is required to form a complete set. For a $N \times 1$ random vector $\mathbf{x}$ we may write equation (6.6) in terms of a linear combination of orthonormal basis vectors $\mathbf{w_i} = (w_{i1}, wi2, \ldots, wiN)^T$ as

$$x_k = \sum_{i=1}^{N} y_i w_{ik} \quad k = 1,2,\ldots,N \tag{6.8}$$

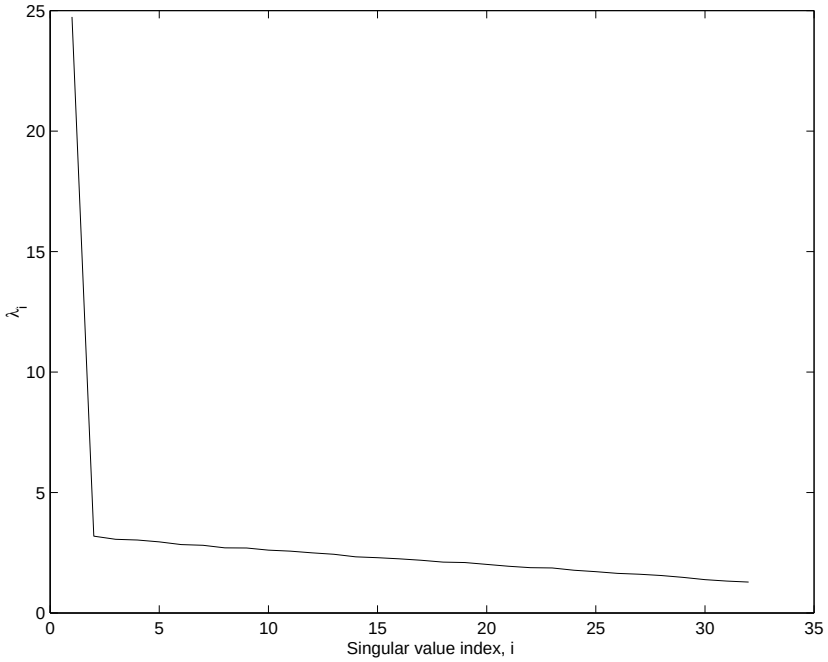

Figure 6.2: Spectrum of singular values for the data in Figure 6.1.

which is equivalent to

$$\mathbf{x} = \mathbf{W}\mathbf{y} \tag{6.9}$$

where $\mathbf{W} = (\mathbf{w_1}, \mathbf{w_2}, \ldots, \mathbf{w_N})$. Now only N basis vectors are required for completeness. The KL transformation or, as it is also often called, the KL transformation to principal components, is obtained as

$$\mathbf{y} = \mathbf{W^T}\mathbf{x} \tag{6.10}$$

where $\mathbf{W}$ is determined from the covariance matrix $\mathbf{C_x}$ of the process

$$\mathbf{C_x} = \mathbf{W}\mathbf{\Lambda}\mathbf{W^T} \tag{6.11}$$

Let us now turn our attention to the problem of the KL transformation for multivariate statistical analysis. In this case we consider M vectors $\mathbf{x_i}, \mathbf{i} = \mathbf{1}, \mathbf{M}$ arranged in a $M \times N$ data matrix $\mathbf{X}$. The M rows of the data matrix are viewed as M realizations of the

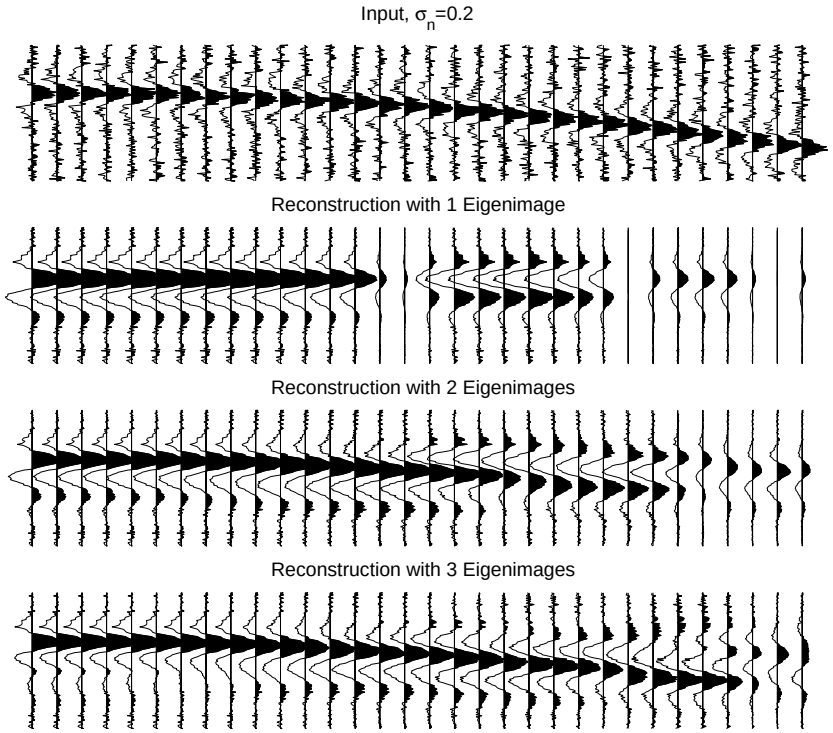

Figure 6.3: A Parabolic event immersed in nose and the reconstruction by means of the 1,2 and 3 eigenimages

stochastic process $\mathbf{x}$ and consequently the assumption is that all rows have the same row covariance matrix $\mathbf{C_r}$. The KL transform now becomes

$$\mathbf{Y} = \mathbf{W^T X} \tag{6.12}$$

An unbiased estimate of the row covariance matrix is given by

$$\hat{\mathbf{C}}_\mathbf{r} = \frac{1}{M-1} \sum_{i=1}^{M} \mathbf{x_i x_i^T} \tag{6.13}$$

assuming a zero mean process for convenience. Since the factor $M-1$ does not influence the eigenvectors, we can see from equation (12) and the definition of $\mathbf{U}$ that $\mathbf{W} = \mathbf{U}$. Consequently, we can rewrite equation (11) as

$$\mathbf{Y} = \mathbf{U^T X} \tag{6.14}$$

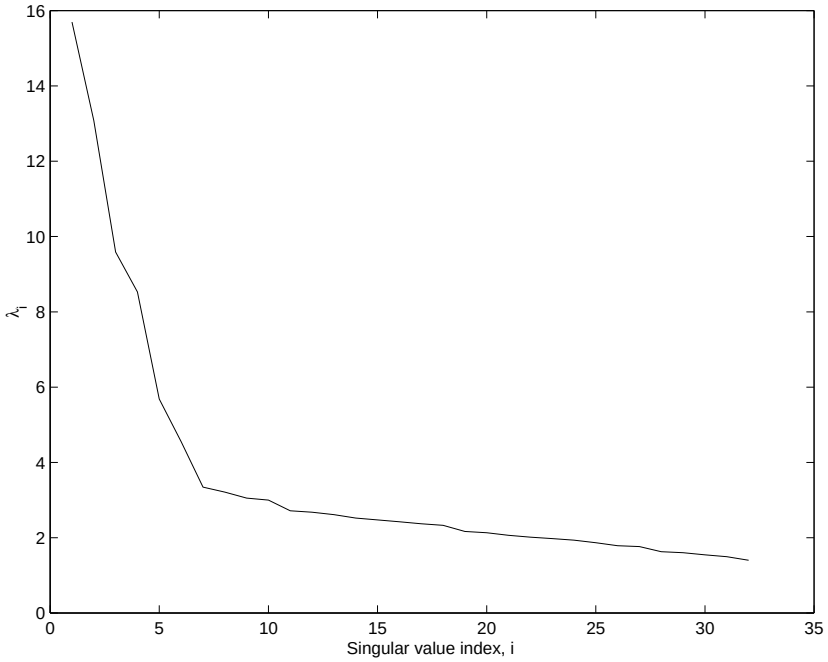

Figure 6.4: Spectrum of singular values for the data in Figure 6.3.

Substituting equation (6.1) into equation (6.14), we obtain

$$\mathbf{Y} = \mathbf{U}^T\mathbf{U}\Sigma\mathbf{V}^T = \Sigma\mathbf{V}^T \tag{6.15}$$

The principal components contained in the matrix $\mathbf{Y}$ may be viewed as the inner product of the eigenvectors of $\mathbf{XX^T}$ with the data, or as the weighted eigenvectors of $\mathbf{X^TX}$.

Since $\mathbf{X}$ may be reconstructed from the principal component matrix $\mathbf{Y}$ by the inverse KL transformation

$$\mathbf{X} = \mathbf{UY} \tag{6.16}$$

we may combine last two equations to obtain

$$\mathbf{X} = \mathbf{U\Sigma Y^T} \tag{6.17}$$

Last equation is identical with equation (6.1), showing that, providing we are considering a multivariate stochastic process, the SVD and the KL transformation are computationally equivalent.

6.2 Eigenimage analysis of common offset sections

We investigate the application of eigenimage analysis to common offset sections. Our principal goal is to show that often, common offset sections can be efficiently compressed using eigenimages. A subsidiary goal is to improve the S/N ratio of pre-stack data by eigenimage filtering of common offset sections.

We consider the data matrix X to be composed of n_x traces with n_t data points per trace, the n_x traces forming the columns of X. The Singular Value Decomposition (SVD) of X (Lanczos, 1961), is given by:

$$X = \sum_{i=1}^{r} \lambda_i \, u_i \, v_i^T \, , \tag{6.18}$$

where r indicates the rank of the matrix X, u_i is the i-th eigenvector of $X\,X^T$, v_i is the $i-$th eigenvector of $X^T\,X$ and λ_i is the i-th singular values of X. Andrew and Hunt (1977) called the outer product $u_i\,v_i^T$ the i-th eigenimage of the matrix X.

Suppose that X represents a seismic section and that all the n_x traces are linearly independent. In this case the matrix X is of full rank and all the singular values are different from zero. A perfect reconstruction of X requires all eigenimages. On the other hand, in the case where all n_x traces are equal to within a scale factor, all traces are linearly dependent, X is of rank one and may be perfectly recovered by the first eigenimage, $\lambda_1 u_1\,v_1^T$.

The eigenimage decomposition can be used to optimally extract laterally coherent waveforms. In general, common offset sections exhibit a good lateral coherence. Our approach in this paper is to first decompose the pre-stack data cube into common offset sections and then apply eigenimage analysis to compress each common offset section and improve the S/N ratio.

Our strategy is summarized as follows:

1. The pre-stack data cube is decomposed into common offset sections, in our examples we construct 10 common offset sections containing traces with offsets indicated in Table 1.

2. Each common offset section is decomposed into eigenimages. 3- Only the eigenvectors that correspond to the first p singular values are kept.

3. Equation (6.18) is used to reconstruct the common offset section. If the misfit is acceptable, we save the vectors u_i, v_i, λ_i, $i = 1 \ldots p$.

It is interesting to note that the amount of data compression that can be achieved using this procedure is remarkably high. Using the SVD we can represent each common offset section by n_2 floats:

$$n_2 = p \times n_t + p \times n_x + p\,.$$

We define the compression ratio as follows

$$C = (n_1 - n_2)/n_2,$$

where $n_1 = n_x \times n_t$ is the total number of floats required to represent the common offset section, X.

In Table 1 we summarize the compression ratio for the ten common offset sections in which we have decomposed the data cube. In this example p corresponds to the number of singular values that account for 30% of the total power encountered in the spectrum of singular values. In Figure 6.51 we portray the spectra of singular values. We note that the eigen-decomposition is in terms of a few energetic singular values that correspond to coherent events in the common offset domain.

COS#	Offset [m]	p	$C = (n_1 - n_2)\,/\,n_2$
1	0-221	9	13.7
2	221-427	6	20.0
3	427-633	4	18.7
4	633-839	5	17.8
5	839-1045	4	23.7
6	1045-1250	5	21.2
7	1250-1456	6	18.2
8	1456-1662	6	14.4
9	1662-1868	6	15.2
10	1868-2780	7	13.0

Table 6.1: Compression ratios for 10 common offset sections. The variable p indicates the number of singular values used in the eigen-decomposition.

In Figures 6.6 and 6.7 we display the common offset section #2 after and before eigen-image filtering. Since the evenst are fairly flat, we can always retain the information content of the section in a few eigenimages. compression and S/N ratio enhancement

In Figures 6.8 and 6.9 we display a CDP after and before performing the eigenimage analysis in common offset domian. It is clear that we cannot use eigenimages in the CDP domain, but after filtering in the common offset domain an sorting in CDPs we note that some high frequency noise at near offset traces was eliminated.

In summary, by sorting the data into common offset section we have been able to apply the eigenimage analysis on individual common offset traces. The pre-stack volume is reconstructing with a minimal distortion.

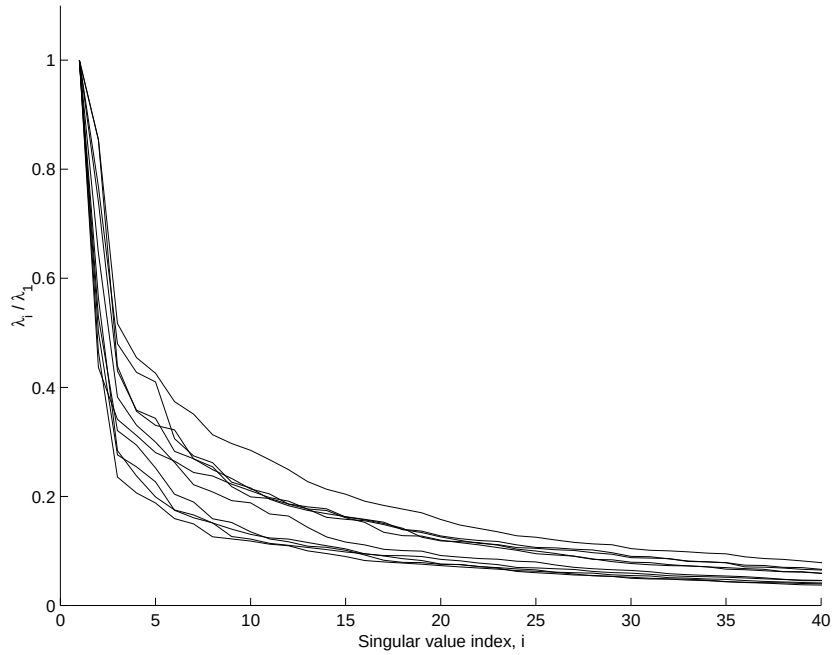

Figure 6.5: Spectra of singular values for the 10 common offset sections used to test the algorithm.

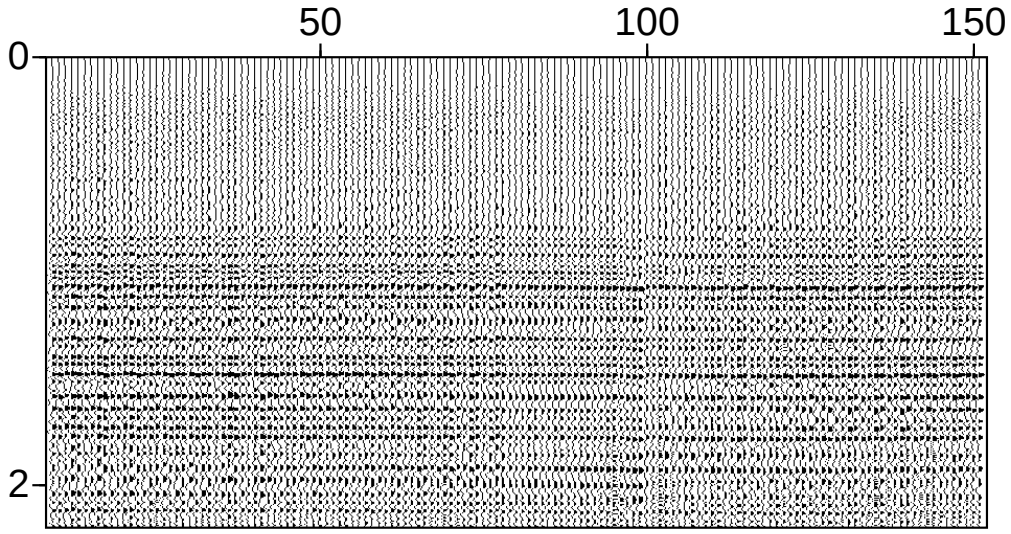

Figure 6.6: Common offset section #2.

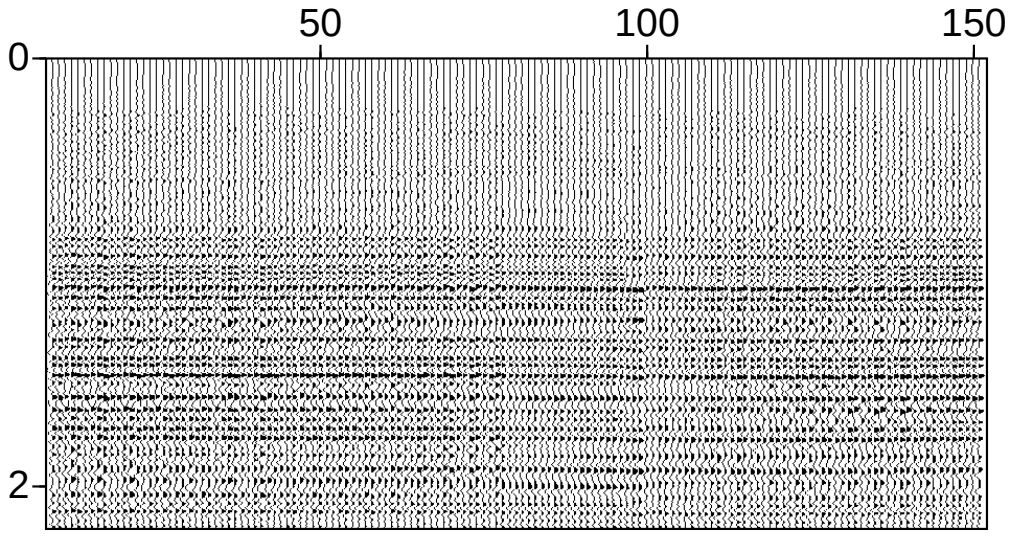

Figure 6.7: Common offset section #2 after eigenimage filtering

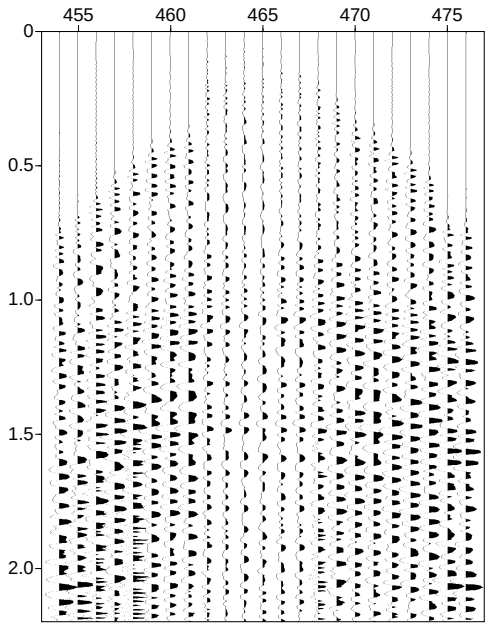

Figure 6.8: Original CDP.

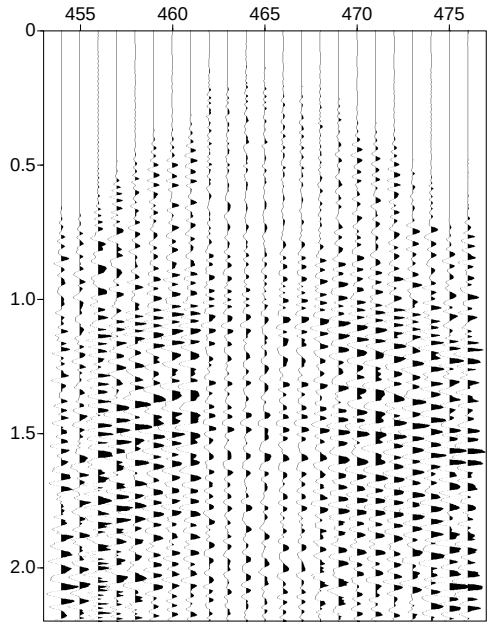

Figure 6.9: CDP after Eigenimage filtering in the common offset domain

6.2.1 Eigenimages and application to Velocity Analysis

Eigen-decomposition of seismic data (hyperbolic windows in CMP gathers) can be used to design coherence measures for high resolution velocity analysis. The idea is to replace the semblance measure by a norm that is a function of the eigenvalues of the covariance matrix of the gate of analysis. In this section we will derive a very simple algorithm that can be used to compute high resolution coherence measures for velocity analysis.

Techniques that exploit the eigen-structure of the covariance matrix have been borrowed from the field of array processing (Bienvenu and Kopp, 1983; Wax et al., 1984), and applied to velocity analysis by different researchers (Biondi and Kostov, 1989; Key and Smithson, 1990; Kirlin, 1992).

The seismic signal, in the presence of noise, at receiver i may be modeled using the following equation:

$$x_i(t) = s(t - \tau_i) + n_i(t) \qquad i = 1, N\,, \tag{6.19}$$

where $\tau_i = (t_0^2 + d_i^2/v^2)^{1/2} - t_0$ is the delay of the signal between the i-th receiver and a receiver having $d_0 = 0$. If a waveform is extracted along a hyperbolic path parametrized with velocity v, equation (6.19) may be rewritten as

$$x_i(t) = s(t) + n_i(t) \qquad i = 1, N\,, \tag{6.20}$$

noindent where, to avoid notational clutter, I used the same variable $x(t)$ to designate the delayed waveform (equation (6.19)) and the corrected waveform (equation (6.20)). The covariance matrix of the the signal is defined as:

$$R_{i,j}(t) = E[x_i(t)x_j(t)] \qquad i, j = 1, N\,, \tag{6.21}$$

where E denotes the expectation operator. If we assume the noise and signal to be uncorrelated the data covariance matrix becomes:

$$R_{i,j}(t) = R_{si,j}(t) + \sigma_n^2(t)\delta_{i,j}\,, \tag{6.22}$$

where $R_{si,j}(t)$ denotes the signal covariance matrix, and $\delta_{i,j} = 1$, if $i = j$ and $\delta_{i,j} = 0$, otherwise. Assuming a stationary source and a stationary noise process, we may drop the dependence on t. It is easy to verify that the eigenvalues of the covariance matrix become

$$\lambda_i = \lambda_{si} + \sigma_n^2 \qquad i = 1, 2, \ldots, N\,, \tag{6.23}$$

where λ_{si} are the eigenvalues of the signal covariance matrix. Assuming that the signal is invariant across each trace, the signal covariance matrix is rank 1, and we can write the following relationships:

$$\begin{aligned} \lambda_{s1} &= N.P_s \\ \lambda_{si} &= 0 \qquad i = 2, ..., N\,, \end{aligned} \tag{6.24}$$

where $P_s = E[s(t)^2]$ denotes the signal power. Using equation (6.23), the eigenvalues of the data covariance matrix become

$$\begin{aligned} \lambda_1 &= N.P_s + \sigma_n^2 \\ \lambda_i &= \sigma_n^2 \quad i = 2, ..., N\,. \end{aligned} \tag{6.25}$$

For uncorrelated noise, the minimal $N-1$ eigenvalues of the data are equal to the variance of the noise. The largest eigenvalue is proportional to the power of energy of the coherent signal plus the variance of the noise.

In real situations, the eigen-spectrum is retrieved from an estimate of the data covariance matrix. If the stationary random processes $x_i(t)$ and $x_j(t)$ are ergodic the ensemble averages defined in equation (6.21) can be replaced by time averages (see for instance, Bendat and Piersol, 1971). The estimator of the covariance matrix becomes:

$$\hat{R}_{i,j} = \frac{1}{2M+1} \sum_{k=-M}^{M} x_i(k\Delta t) x_j(k\Delta t)\,. \tag{6.26}$$

Using the results given in equations (6.24) and (6.25) it is evident that an estimator of the noise variance is

$$\hat{\sigma}_n^2 = \frac{1}{N-1} \sum_{i=2}^{N} \hat{\lambda}_i\,. \tag{6.27}$$

Similarly, an estimator of the signal energy is given by

$$\hat{P}_s = \frac{\hat{\lambda}_1 - \hat{\sigma}_n^2}{N}\,, \tag{6.28}$$

and equations (6.27) and (6.28) can be combined into a single measure, the signal-to-noise-ratio:

$$\widehat{C} = \frac{1}{N} \frac{\hat{\lambda}_1 - \sum_{i=2}^{N} \hat{\lambda}_i/(N-1)}{\sum_{i=2}^{N} \hat{\lambda}_i/(N-1)} \,. \tag{6.29}$$

The coherence measure, $\hat{C}$, was devised assuming the presence of a signal and that the proper velocity is used to extract the waveform. In general the coherence ,$\hat{C}$, is computed for different gates and different trial velocities. It is convenient to explicitly emphasize the dependence of the coherence on these parameters by denoting $\hat{C}(t_0, v)$. When the gate of analysis contains only noise, the measure $\hat{C}(t_0, v)$ tends towards zero. When the trial velocity does not match the velocity of the reflection, it is not possible to decompose the eigen-structure of the data into signal and noise contributions. In this case, the covariance matrix has a complete set of eigenvalues different from zero; therefore it is not possible to recognize which part of the eigen-spectrum belongs to the noise and which belongs to the signal process.

Key and Smithson (1990) proposed another coherence measure based on a log-generalized likelihood ratio which tests the hypothesis of equality of eigenvalues,

$$\hat{W}_{ml} = M \log^N \left[\frac{(\sum_{i=1}^{N} \hat{\lambda}_i/N)^N}{\prod_{i=1}^{N} \hat{\lambda}_i} \right] . \tag{6.30}$$

In the absence of signal, $\lambda_i = \sigma_n^2$, $i = 1, N$ and hence $W_{ml} = 0$. In the presence of a single reflected signal, $\lambda_1 \neq 0$, $\lambda_i = 0$, $i = 2, N$ and $W_{ml} \to \infty$. Therefore, W_{ml} provides a strong discrimination between signal and noise. Key and Smithson (1990) combined equation (6.29) and (6.30) into a single measure, K_{ml}, given by the product:

$$\hat{K}_{ml} = \hat{W}_{ml}\, \hat{C} \,. \tag{6.31}$$

It is important to point out that only one eigenvalue, λ_1, is required to estimate the coherence measure, $\hat{C}$. Since

$$Trace(\hat{\mathbf{R}}) = \hat{\lambda}_1 + \hat{\lambda}_2 + \ldots + \hat{\lambda}_N \tag{6.32}$$

where

$$Trace(\hat{\mathbf{R}}) = \sum_{i=1}^{N} \hat{R}_{ii} \,. \tag{6.33}$$

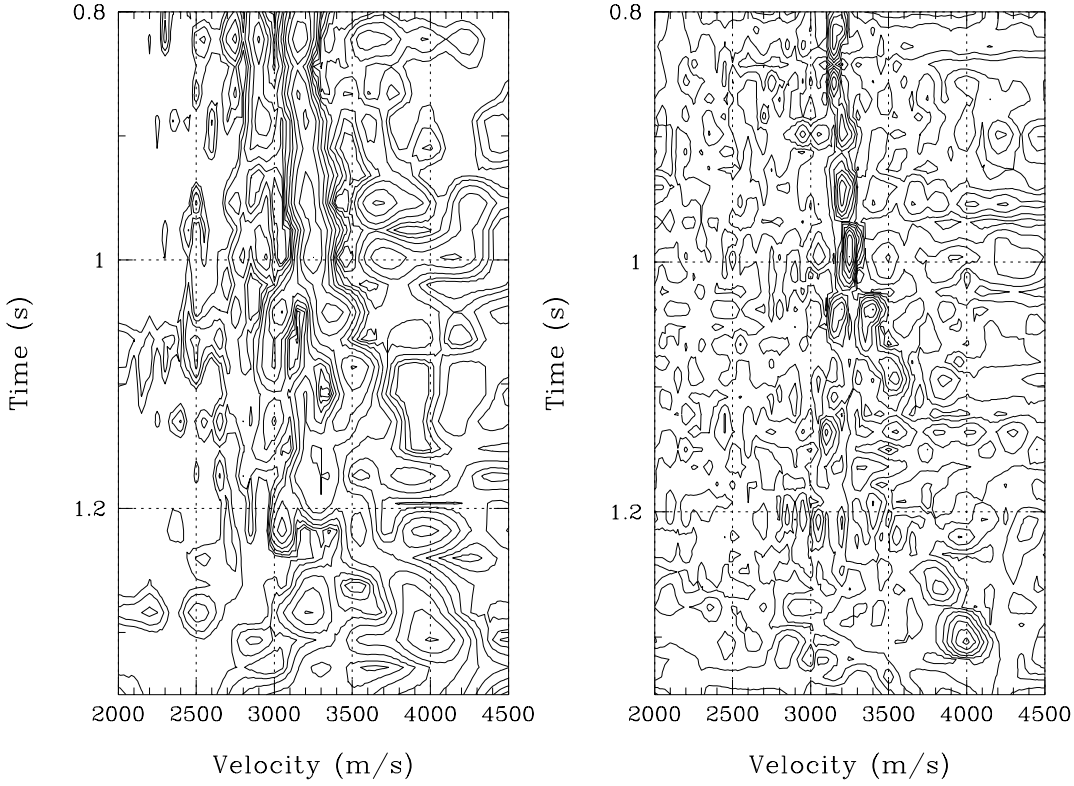

Figure 6.10: Left: Semblance of a CMP gather. Right: High resolution coherence analysis (SNR measure).

It is easy to see from equations (6.32) and (6.33) that only $\hat{\lambda}_1$ is needed to compute the coherence measure, $\hat{C}$.

It is also important to mention that the velocity panel obtained via the SNR coherence measure can be further improved by adopting a bootstrap procedure (Sacchi, 1998). In this case, the seismic traces are randomly sampled to produce individual estimates of the coherence measure. From this information one can obtained an average coherence measure and a histogram (in fact a density kernel estimator) of the position of the peak that optimizes the coherence. The improve SNR coherence obtained with this techniques is portrayed in Figure (6.11).

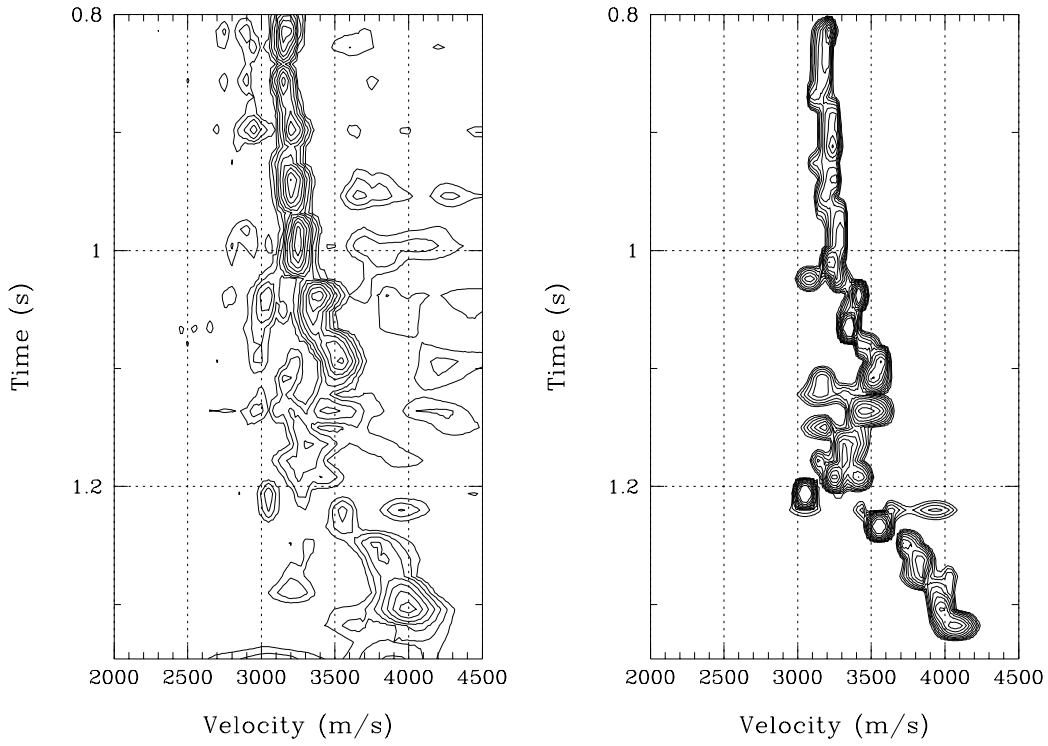

Figure 6.11: Left: Average SNR measure obtained via bootstrapping individual realizations. Right: Frequency distribution of the peak that maximizes the coherence after 50 bootstrap realizations.

6.3 A Matlab Code for Eigenimage Analysis

```
% A Code to filter data using the Eigenimage approach

% Generation of the model. Single
% event with parabolic moveout.

dt = 4./1000; w = ricker(20.,dt); nw=max(size(w));
nx = 32; nt = 128;
DATA = zeros(nx,nt);

for i=1:nx
 for j=1:nw
   c= fix(0.05*i*i);
  DATA(i,20+j+c) = w(j);
 end
end

% Add noise to the model
NOISE = 0.2 * randn(nx,nt);
DATA = DATA + NOISE;


[U S V] = svd(DATA);

% Reconstruction with 3 eigenimages

 p = 4;    % Keep 1,2,3.
 q = min(size(S));
 for i = p:q;
 S(i,i) = 0;
 end

% Filtered image
 DATA = U*S*V';
```

6.3.1 References

Andews, H. C., and Hunt, B. R., 1977, *Digital image restoration*, Prentice-Hall, Signal Processing Series.

Bienvenu, G., and Kopp, L., 1983, Optimality of high resolution array processing using the eigensystem approach: IEEE, Trans. Acoust., Speech, Signal Processing., **ASSP-31**, 1235-1248.

Biondi, B. L., and Kostov, C., 1989, High-resolution velocity spectra using eigenstructure methods: Geophysics, **54**, 832-842.

Key, S. C., and Smithson, S. B., 1990, New approach to seismic-event detection and velocity determination: Geophysics, **55**, 1057-1069.

Kirlin, R. L., 1992, The relationship between the semblance and the eigenstructure velocity estimators, Geophysics: **57**, 1027-1033.

Freire, S.L.M and Ulrych, T.J., 1988, Application of singular value decomposition to vertical seismic profiling, Geophysics, **53**, 778-785.

Hemon, C.H. and Mace, D., 1978, Essai d'une application de la transformation de Karhunen-Loève au traitement sismique, Geophysical Prospecting, **26**, 600-626.

Jones, I.F. and Levy, S., 1987, Signal-to-noise ratio enhancement in multichannel seismic data via the Karhunen-Loève transform, Geophysical Prospecting, **35**, 12-32.

Lanczos, C., 1961, *Linear Differential operators*, D. Van Nostrand Co.

Sacchi, M.D., 1998, A bootstrap procedure for high-resolution velocity analysis: Geophysics, **65**, 1716-1725.